Monte Carlo simulation on ferroelectric response to magnetic field in an elastic Ising spin chain

Xiaoyan Yao (姚晓燕),[1,a)] Veng Cheong Lo (羅永祥),[2] and Jun-Ming Liu (刘俊明)[3]
[1]*Department of Physics, Southeast University, Nanjing 211189, China*
[2]*Department of Applied Physics, The Hong Kong Polytechnic University, Hong Kong, China*
[3]*Nanjing National Laboratory of Microstructures, Nanjing University, Nanjing 210093, China*

(Received 19 February 2009; accepted 16 May 2009; published online 1 July 2009)

The fantastic ferroelectric response to the magnetic field observed in Ca_3CoMnO_6 compound, where the ferroelectricity is driven by the collinear magnetism, is investigated by using Monte Carlo simulation based on a one-dimensional elastic Ising model. The microscopic domain structures of spins and ionic displacements are evaluated at different temperatures under different external magnetic fields. It is revealed that the up-up-down-down ($\uparrow\uparrow\downarrow\downarrow$) spin domains clamped with the domains of ionic displacement are responsible for the exotic ferroelectric behavior upon different magnetic fields in the low temperature range. © *2009 American Institute of Physics*.
[DOI: 10.1063/1.3153113]

I. INTRODUCTION

Spin frustration has attracted considerable attention in the physics of strongly correlated systems in recent years. The competing interactions in the frustrated compounds produce a high degeneracy of states due to spin frustration and consequently peculiar magnetic phenomena such as spin ice,[1,2] spin glass,[3] and spin liquid[4,5] as well as the multistep magnetization.[6–9] Recently the discovery of magnetism-driven ferroelectricity in the frustrated magnet rejuvenated the interest of investigation in both fields of spin frustration and multiferroicity.[10–14] In multiferroic compounds, the frustration plays the role to induce spatial variations in magnetization, which break the special inversion symmetry and thus produce ferroelectricity. Due to the magnetic origin of ferroelectricity, the electric polarization (P) and the dielectric constant (ε) in these materials are highly sensitive to the applied magnetic field (h), making these multiferroic systems attractive in applications. On the other hand, the frustration also brings new challenge to the theory of multiferroicity. In different structures it produces a variety of complex magnetic phases and a series of transitions, which result in very complicated magnetoelectric coupling and puzzling phenomena. The corresponding microscopic mechanism, essential to achieve their potential applications, is still a challenging task.

One-dimensional (1D) Ising spin chain with the competing nearest-neighbor and next-nearest-neighbor interactions, which is a typical spin frustration system, demonstrates various commensurate magnetic phases.[15] It was predicted that the up-up-down-down collinear spin order observed in this model will induce ferroelectricity by the exchange striction,[10] which is very different from the noncollinear-magnetism-driven ferroelectricity.[16–18] This prediction was remarkably substantiated by the experiment of Choi *et al.*[19] It was reported that the ferroelectricity induced by the collinear spin order had been discovered in $Ca_3Co_{2-x}Mn_xO_6$ ($x \approx 0.96$, very near one). Ca_3CoMnO_6 belongs to the family of triangular spin-chain compounds with the general formula A'_3ABO_6 (where A' is Ca or Sr and A and B are transition metal elements). It is composed of parallel 1D $CoMnO_6$ chains aligned along the hexagonal c-axis, separated by A'^{2+} ions, forming a triangular lattice in the ab-plane.[20] Every $CoMnO_6$ chain consists of the alternatively face-sharing CoO_6 trigonal prisms and MnO_6 octahedra. 1D Ising model can be used to characterize this compound due to its quasi-1D magnetic structure and the strong Ising-like anisotropy.[19–21]

The collinear-magnetism-driven ferroelectricity observed in Ca_3CoMnO_6 attracts a lot of attention. By the density functional theory and *ab initio* electronic structure calculations, Wu *et al.*[21] and Zhang *et al.*,[22] respectively, confirmed that the inequivalence of the Co–Mn distances in an up-up-down-down spin order accounts for the ferroelectricity. By using Monte Carlo (MC) simulation based on a 1D elastic Ising model, the present authors reproduced the temperature-dependent ferroelectric and magnetic behaviors in the low temperature (T) range. The simulation results are in qualitative agreement with the experimental data of Ca_3CoMnO_6.[23,24] It is revealed that the macroscopic P induced by the ionic displacements is attributed to the exchange striction in an up-up-down-down spin order. Moreover, the freezing and melting phenomena of P against T were discussed in detail at a microscopic level. However the puzzling ferroelectric response to magnetic field, especially the crossover behavior of $P(T)$ curves under different magnetic fields, and its microscopic mechanism remain unresolved. In this paper, we perform extensive simulation on the 1D elastic Ising model to gain an insight into the microscopic scenario of the ferroelectric response to h. In particular, the microscopic domain structures of spins and ionic displacements are discussed in detail to unveil the coupling between magnetism and ferroelectricity. It is indicated that the up-up-down-down spin domain (UDSD) clamped with the ionic displacement domain (IDD) through the exchange

a)Electronic mail: yaoxiaoyan@gmail.com.

striction induces the exotic magnetic response of ferroelectric behavior.

II. MODEL AND SIMULATION

The Hamiltonian for this 1D elastic Ising spin chain can be written as

$$H = -\sum_{\langle i,j\rangle} J_{\mathrm{FM}}(r_{ij}) S_i S_j - \sum_{[i,k]}^{\mathrm{Mn}} J_{\mathrm{AFMn}} S_i S_k - \sum_{[i,k]}^{\mathrm{Co}} J_{\mathrm{AFCo}} S_i S_k - hg\mu_B \sum_i S_i - E\sum_i q d_i + \frac{1}{2} k \sum_i d_i^2, \quad (1)$$

where $S_i = \pm 1$ represents the spin at the ith site of the chain. The first term on the right of Eq. (1) is the ferromagnetic (FM) energy, where $\langle i,j\rangle$ denotes the summation over all the nearest-neighboring spin pairs. J_{FM} depends on the distance between the two nearest-neighboring spins due to exchange striction. It can be expanded to the following linear approximation form:

$$J_{\mathrm{FM}}(r_{i,i+1}) = J_{\mathrm{FM0}}\left(1 + \eta \cdot \frac{r_{i,i+1} - r_0}{r_0}\right) = J_{\mathrm{FM0}}[1 + \eta(d_{i+1} - d_i)], \quad (2)$$

where J_{FM0} is defined as the bare FM spin-spin interaction ($J_{\mathrm{FM0}} > 0$) and η gives the strength of the coupling between the spins and the displacements. $\eta < 0$ reflects that the interaction gets stronger as the spins get closer to each other. r_0 is the original distance between two ions without the exchange striction; $r_{i,i+1}$ is the distance between the ith ion and the $(i+1)$th ion under the exchange striction. d_i denotes the displacement of the ith ion normalized by r_0, and it bears a positive value when this ith ion is approaching the $(i+1)$th one. Therefore, the exchange striction plays the role to shrink the bond lengths between the parallel spins and stretch those between the antiparallel ones, inducing the movements of ions along the chain. According to Eq. (2), the change in J_{FM} is only related to the distance between these two nearest-neighboring spins; therefore the relative movement of these two ions is the key for the exchange striction. For simplicity, it is assumed that only Co ions move, namely, $d_i \neq 0$ for mobile Co ion, but $d_i = 0$ for immobile Mn case.

The second and third terms on the right of Eq. (1) are antiferromagnetic (AFM) energy between the next-nearest-neighboring pairs calculated for Mn and Co, respectively, where $[i,j]$ signifies the summation over all the next-nearest-neighboring pairs. The AFM coupling between each next-nearest-neighboring Mn–Mn pair is stronger than that for Co–Co, namely, $J_{\mathrm{AFMn}} < J_{\mathrm{AFCo}} < 0$.[22] The fourth term is the magnetic field energy, where h is the external magnetic field, g is the Lande factor, and μ_B is the Bohr magnetron. The fifth term denotes the electric energy, where E is the electric field applied along the chain. q is the charge state of the moving ions, that is, $q=2$ for Co^{2+}. The last term on the right of Eq. (1) is the elastic energy presented in the form of harmonic potential, where k is the elastic constant with a value large enough to ensure small values of ionic displacements. For convenience, Boltzmann's constant k_B is chosen to be unity, which means that temperature is measured in energy units and the same units can be used for the exchange coupling and other physical constants. Since the real values of the parameters are not available from experiments, they are chosen by the qualitative comparison between the simulated results and the experimental data, which had been discussed in Ref. 23. The values of these parameters for the simulation are shown in Table I.

TABLE I. System parameters chosen for the simulation.

Parameter	Value
J_{FM0}	90
J_{AFMn}	−65.7
J_{AFCo}	−7.3
η	−8
k	34 000
g	2

It is known that the up-up-down-down spin state with alternating ionic order is very important for the emergence of P. However, it was observed that the up-up-down-down order is actually short-ranged.[19] Therefore, the evolution of UDSD should be focused as a key to understand the properties of the system. As shown in Figs. 1(a) and 1(b), there are two ways to combine the up-up-down-down spin order with the ionic charge order, which give rise to the opposite ionic diaplacement.[19] Correspondingly the UDSD can be divided into two classes, namely, positive UDSD with positive displacement $d_i > 0$ and negative UDSD with $d_i < 0$. The number of the positive UDSD (PUDN) and that of the negative UDSD (NUDN) are counted for different domain size (n_s). Here n_s is defined as the number of separate parallel spin pairs with opposite spins on the neighboring sites, for example, $n_s = 1$ in Fig. 1(c) and $n_s = 2$ in Fig. 1(d). The evolution of PUDN and NUDN for different n_s against T presents the useful information on the T-dependent spin structure. On the other hand, in order to explore the microscopic picture of the ferroelectric polarization, the number of positive displacement domain (PDDN) and that of negative displacement domain (NDDN) are enumerated, respectively, for the different displacement domain's sizes (n_d), where n_d is defined as the amount of the neighboring mobile ions with

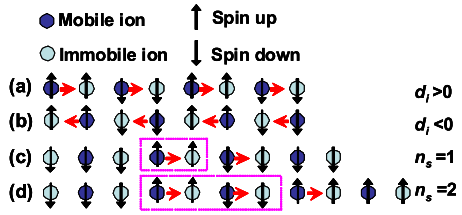

FIG. 1. (Color online) The up-up-down-down Ising spin chain combining with the alternating ionic order in two ways sketched in (a) with ionic displacement of $d_i > 0$ and (b) with $d_i < 0$. (c) An ionic chain with an UDSD of $n_s = 1$ since there is only one separate spin pair as marked by a dotted box. (d) An ionic chain with an UDSD of $n_s = 2$, namely, there are two separate spin pairs presented in a dotted rectangle. All the directions of displacement for the mobile ions have been shown as the arrows. The other mobile ions without arrow have not certain displacement direction because their left and right neighbors have the same spin orientations to it. Therefore their displacements are always too small.

positive displacements lager than 0.01 for the positive IDD or with negative displacements smaller than −0.01 for the negative one. The evolution of UDSD and IDD under different h presents more information on the correlation between the magnetism and the ferroelectricity at a microscopic level

The MC simulation for this 1D Ising spin chain is performed with a system size of $L=4000$ and periodic boundary condition. The spin and the displacement are updated according to the Metropolis algorithm, respectively. Similar to the measurement process in the experiment,[19] the system is initially polarized by a large electric field of $E_0=160$ at low temperature ($T=1$). After E_0 has been removed, P, magnetization (M), and dc magnetic susceptibility ($\chi=M/h$) are calculated with T increasing under a small electric field of $E=1$. Here P is evaluated by summing all the ionic displacements multiplied by the charge of them. For every T, the initial 300 000 MC steps (MCSs) are discarded for equilibration, and then the results are calculated by averaging 10 000 data. Each datum is collected at every 5 MCSs. The final results are obtained by averaging more than ten independent data sets obtained by selecting different seeds for random number generation.

III. RESULTS AND DISCUSSION

As replotted in Fig. 2(a), the experimental results show the complicated ferroelectric and magnetic behaviors under different h.[19] At low T a macroscopic P emerges after the system has been polarized by a high electric field. With increasing T, P rapidly falls at first and then undergoes a gradual decline. When P disappears, a broad peak of $\chi(T)$ curve emerges under a weak magnetic field, and a small peak at low temperature is also observed. The magnetic field has an exotic influence on P, namely, with increasing T, h suppresses P at first and then enhances it; thus a crossover of $P(T)$ curves under different h are displayed. As illustrated in Fig. 2(b), the simulation results qualitatively reproduces the main features of ferroelectric and magnetic behaviors of Ca_3CoMnO_6. Moreover, our simulation exhibits the T-dependent M under different h, as demonstrated in Fig. 2(c). A stepwise behavior is presented, and for each $M(T)$ curve there are three anomalies emerging at three critical temperatures T_1, T_2, and T_3. The first anomaly occurs at about $T_1=1.5$ for different h, where the small peak of $\chi(T)$ curve and the crossover of $P(T)$ curves are observed. The third anomaly appears at about $T_3=4.3$ for different h, which corresponds to the broad peak of χ and the disappearance of P. The second anomaly takes place at different T upon different h, that is, T_2 shifts from 3.4 to 2.8 with h rising from one to four.

In order to comprehend the T-dependences of M and P under different h at a microscopic level, the evolutions of UDSD and IDD are demonstrated in Figs. 3 and 4, respectively. It is seen that Figs. 3(a)–3(h) are similar to Figs. 4(a)–4(h), which means that the response of UDSD to h has a direct influence on the microscopic ionic displacements. This is due to that the ionic displacements are just originated from the exchange striction in the short-ranged up-up-down-down spin state. For example, an UDSD with $n_s=1$ produces

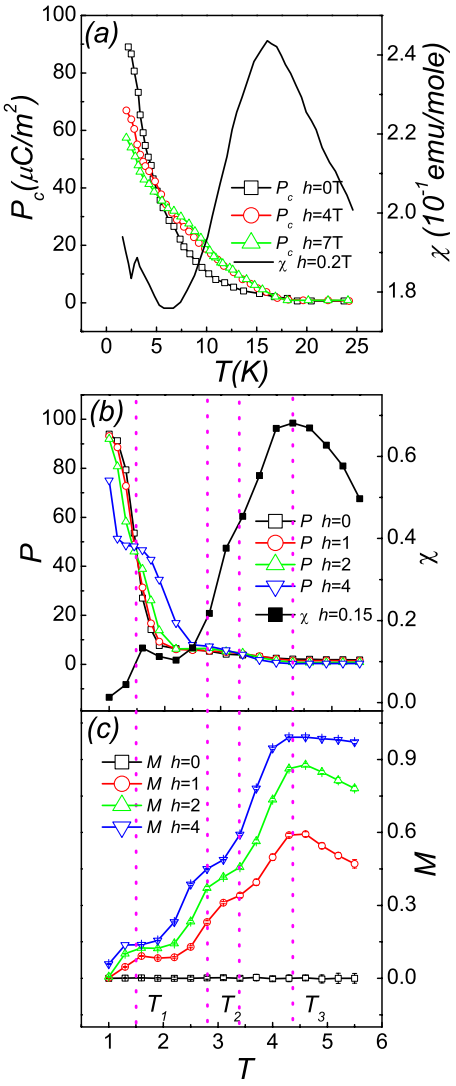

FIG. 2. (Color online) (a) The temperature dependences of electric polarization along the chain direction (P_c) and dc magnetic susceptibility (χ) of single crystal $Ca_3Co_{1-x}Mn_xO_6$ ($x=0.96$) are reproduced from the experimental results in Ref. 19. Here P_c (T) curves were taken under magnetic fields of $h=0$, 4, and 7 T. $\chi(T)$ curve was obtained upon $h=0.2$ T. The simulation results are presented in (b) and (c). (b) The $P(T)$ curves under $h=0$, 1, 2, and 4, and $\chi(T)$ curve upon $h=0.15$. (c) M against T under $h=0$, 1, 2, and 4. The dotted lines mark the positions of the critical temperatures T_1, T_2, and T_3.

an IDD with $n_d=2$ [Fig. 1(c)], an UDSD with $n_s=2$ induces an IDD with $n_s=3$ [Fig. 1(d)], and so on. Therefore, the clamping between the ferroelectric domains and the short-ranged up-up-down-down order induces the one-to-one correspondence between the behaviors of UDSD and IDD.

The T-dependences of M and P, especially the crossover behavior of $P(T)$ curves under different h, can be understood in this scenario of microscopic domains. The macroscopic P is directly related to the result of PDDN minus NDDN. As shown in Fig. 4, for $h=0$ and $T=1$ PDDN shows a high value, while NDDN is almost zero, which is induced by the polarizing electric field and maintains at low temperature, even though the polarizing electric field has been removed. In other words, the ionic displacements are frozen in the direction of the polarizing field, which results in a high P. As T is raised, the decrease in PDDN and the increase in NDDN lead to the sharp fall in P. The crossover phenomenon of

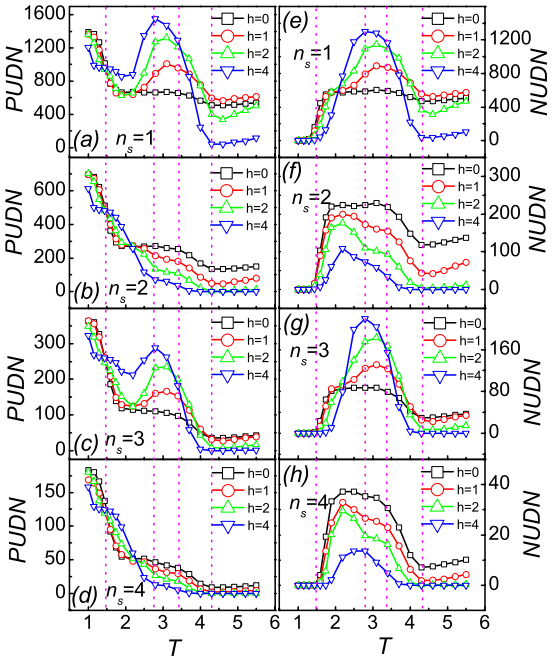

FIG. 3. (Color online) PUDN and NUDN as functions of T under h=0, 1, 2, and 4 for different n_s are displayed respectively. Since PUDN and NUDN obviously decrease for larger n_s, only domain with n_s=1, 2, 3, and 4 are displayed here. [(a)–(d)] PUDN(T) curves under h=0, 1, 2, and 4 for different n_s, namely, from (a) to (d) n_s=1, 2, 3, and 4. [(e)–(h)] NUDN(T) curves upon h=0, 1, 2, and 4 for different n_s, namely, from (e) to (h) n_s =1, 2, 3, and 4. The dotted lines mark the positions of T_1, T_2, and T_3.

$P(T)$ curves under different h can be understood at a microscopic level. A nonzero h suppresses PDDN but hardly affects NDDN below T_1, resulting in the decrease in P with increasing h at a certain T. On the contrary, h enhances PDDN but suppresses NDDN above T_1, and consequently P increases with increasing h. This puzzling response of IDD to h has its magnetic origin. As shown in Fig. 3, the presence of h suppresses PUDN but hardly affects NUDN below T_1. On the contrary, it enhances PUDN but suppresses NUDN above T_1. These behaviors of UDSD are very similar to corresponding IDD curves. It is indicated that h takes effect on UDSD structure, which produces corresponding IDD structure, and the IDD structure decides the value of P. The one-to-one correspondence between the behaviors of UDSD and IDD under different h presents the magnetic origin of the ferroelectric response to h.

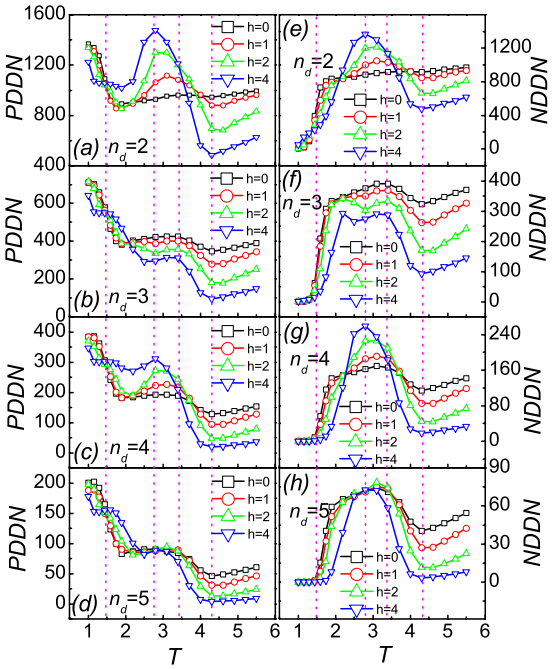

FIG. 4. (Color online) [(a)–(d)] PDDN(T) curves under h=0, 1, 2, and 4 for different n_d, namely, from (a) to (d) n_d=2, 3, 4, and 5. [(e)–(h)] NDDN(T) curves upon h=0, 1, 2, and 4 for different n_d, namely, from (e) to (h) n_d =2, 3, 4, and 5. Here n_d is the size of displacement domain, and the dotted lines mark the positions of T_1, T_2, and T_3.

It is interesting that UDSD with odd or even n_s shows very different responses to h in the T-range about T_2, as presented in Fig. 3, although these responses are similar for different odd n_s (for instance, n_s=1 and 3) or for different even n_s (for instance, n_s=2 and 4). For even n_s, PUDN and NUDN decrease with increasing h at a certain T in this T-range. However for odd n_s, both PUDN and NUDN show broad peaks. As h is raised, the peak height increases and the peak position shifts to a lower T, which corresponds to the different T_2 observed in $M(T)$ curves for different h. The main difference between UDSDs with odd and even n_s is whether the both sides of this UDSD have the same spin orientation, namely, the spin directions on the two sides are the same for odd n_s, but they are opposite for even n_s, as illustrated in Figs. 1(c) and 1(d). When h is applied, the spins are forced to flip to the same direction of h. Thus the UDSDs with odd n_s are enhanced because they have both sides with the spin orientation along the direction of h. Therefore they show a higher peak with increasing h [Figs. 3(a), 3(c), 3(e), and 3(g)], which also results in a anomaly at T_2 displayed in $M(T)$ curves [Fig. 2(c)]. As demonstrated in Fig. 4, IDD also shows odd-even difference in the same T-range, except that odd n_s corresponds even n_d and vice versa. Though PDDN(T) and NDDN(T) with even n_d exhibit a broad peak at about T_2, the highness of PDDN peak is just slightly higher than that of NDDN peak at a certain n_d. The counteraction between them diminishes the peak, and consequently there is no peak in $P(T)$ curve at about T_2. Above T_3, where the transition to paraelectric state occurs, all UDSD and IDD show similar linear behavior. The one-to-one correspondence between UDSD and IDD confirms the magnetic origin of ferroelectricity in this system at a microscopic level. In this scenario, the complicated ferroelectric responses to h can be revealed by the evolution of the microscopic domain structure.

IV. CONCLUSION

In summary, the ferroelectric response to the external magnetic field through the exchange striction in an elastic Ising spin chain is investigated by using MC simulation. In order to understand the complicated magnetoelectric phenomenon observed in Ca_3CoMnO_6, the microscopic pictures of spin configuration and ionic displacement are presented against T at different h. It is demonstrated that h competes with the exchange striction and the frustration, which takes a very complex effect on the up-up-down-down spin order at

different T. The one-to-one correspondence between the behaviors of UDSD and IDD confirms the strong coupling between the spin configuration and the ionic displacements. The exotic behavior of P under different h can be understood in this scenario of domain structure, especially for the crossover of $P(T)$ curves at low T. Although the real material is far more complicated than the present model, the microscopic domain structure revealed in the present work would help to understand the ferroelectric response to h in the frustrated magnet.

ACKNOWLEDGMENTS

This work was supported by the research grants from the National Natural Science Foundation of China (Grant Nos. 10747115 and 10874075).

[1]G. Ehlers, A. L. Cornelius, T. Fennell, M. Koza, S. T. Bramwell, and J. S. Gardner, J. Phys.: Condens. Matter **16**, S635 (2004).
[2]S. T. Bramwell and M. J. P. Gingras, Science **294**, 1495 (2001).
[3]S. R. Dunsiger, R. F. Kiefl, K. H. Chow, B. D. Gaulin, M. J. P. Gingras, J. E. Greedan, A. Keren, K. Kojima, G. M. Luke, W. A. MacFarlane, N. P. Raju, J. E. Sonier, Y. J. Uemura, and W. D. Wu, Phys. Rev. B **54**, 9019 (1996).
[4]J. S. Helton, K. Matan, M. P. Shores, E. A. Nytko, B. M. Bartlett, Y. Yoshida, Y. Takano, A. Suslov, Y. Qiu, J.-H. Chung, D. G. Nocera, and Y. S. Lee, Phys. Rev. Lett. **98**, 107204 (2007).
[5]J. Robert, V. Simonet, B. Canals, R. Ballou, P. Bordet, P. Lejay, and A. Stunault, Phys. Rev. Lett. **96**, 197205 (2006).
[6]X. Yao, S. Dong, H. Yu, and J. Liu, Phys. Rev. B **74**, 134421 (2006).
[7]V. Hardy, M. R. Lees, O. A. Petrenko, D. M. Paul, D. Flahaut, S. Hébert, and A. Maignan, Phys. Rev. B **70**, 064424 (2004).
[8]X. Yao, S. Dong, K. Xia, P. Li, and J.-M. Liu, Phys. Rev. B **76**, 024435 (2007).
[9]X. Yao, S. Dong, and J.-M. Liu, Phys. Rev. B **73**, 212415 (2006).
[10]S.-W. Cheong and M. Mostovoy, Nature Mater. **6**, 13 (2007).
[11]T. Kimura, T. Goto, H. Shintani, K. Ishizaka, T. Arima, and Y. Tokura, Nature (London) **426**, 55 (2003).; K. F. Wang, J.-M. Liu, and Z. F. Ren, Adv. Phys. **58**, 321 (2009).
[12]Y. Yamasaki, S. Miyasaka, Y. Kaneko, J.-P. He, T. Arima, and Y. Tokura, Phys. Rev. Lett. **96**, 207204 (2006).
[13]S. Seki, Y. Yamasaki, M. Soda, M. Matsuura, K. Hirota, and Y. Tokura, Phys. Rev. Lett. **100**, 127201 (2008).
[14]H. Sagayama, K. Taniguchi, N. Abe, T.-H. Arima, M. Soda, M. Matsuura, and K. Hirota, Phys. Rev. B **77**, 220407 (2008).
[15]M. E. Fisher and W. Selke, Phys. Rev. Lett. **44**, 1502 (1980).
[16]H. Katsura, N. Nagaosa, and A. V. Balatsky, Phys. Rev. Lett. **95**, 057205 (2005).
[17]I. A. Sergienko and E. Dagotto, Phys. Rev. B **73**, 094434 (2006).
[18]Q. C. Li, S. Dong, and J.-M. Liu, Phys. Rev. B **77**, 054442 (2008).
[19]Y. J. Choi, H. T. Yi, S. Lee, Q. Huang, V. Kiryukhin, and S.-W. Cheong, Phys. Rev. Lett. **100**, 047601 (2008).
[20]V. G. Zubkov, G. V. Bazuev, A. P. Tyutyunnik, and I. F. Berger, J. Solid State Chem. **160**, 293 (2001).
[21]H. Wu, T. Burnus, Z. Hu, C. Martin, A. Maignan, J. C. Cezar, A. Tanaka, N. B. Brookes, D. I. Khomskii, and L. H. Tjeng, Phys. Rev. Lett. **102**, 026404 (2009).
[22]Y. Zhang, H. J. Xiang, and M.-H. Whangbo, Phys. Rev. B **79**, 054432 (2009).
[23]X. Yao and V. C. Lo, J. Appl. Phys. **104**, 083919 (2008).
[24]X. Yao, V. C. Lo, and J.-M. Liu, J. Appl. Phys. **105**, 033907 (2009).